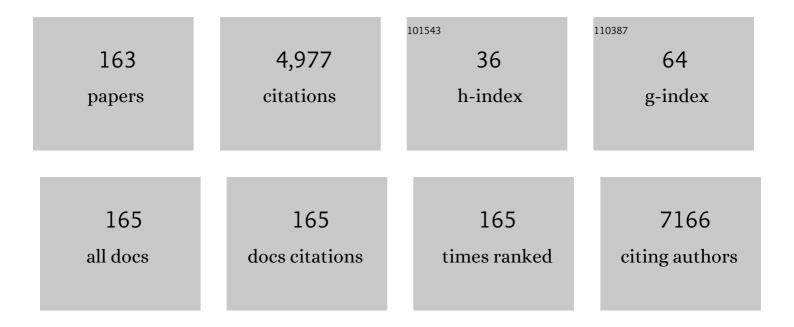
## Rosanna Larciprete

List of Publications by Year in descending order

Source: https://exaly.com/author-pdf/2926452/publications.pdf Version: 2024-02-01



#	Article	IF	CITATIONS
1	Dual Path Mechanism in the Thermal Reduction of Graphene Oxide. Journal of the American Chemical Society, 2011, 133, 17315-17321.	13.7	426
2	Titanium-carbide MXenes for work function and interface engineering in perovskite solar cells. Nature Materials, 2019, 18, 1228-1234.	27.5	418
3	Single-Wall Carbon Nanotube Interaction with Gases:Â Sample Contaminants and Environmental Monitoring. Journal of the American Chemical Society, 2003, 125, 11329-11333.	13.7	261
4	XPS study of the L-CVD deposited SnO2 thin films exposed to oxygen and hydrogen. Thin Solid Films, 2001, 391, 198-203.	1.8	216
5	Oxygen Switching of the Epitaxial Graphene–Metal Interaction. ACS Nano, 2012, 6, 9551-9558.	14.6	195
6	Atomic Oxygen on Graphite: Chemical Characterization and Thermal Reduction. Journal of Physical Chemistry C, 2012, 116, 9900-9908.	3.1	145
7	Transfer-Free Electrical Insulation of Epitaxial Graphene from its Metal Substrate. Nano Letters, 2012, 12, 4503-4507.	9.1	120
8	Direct observation of excimer-laser photoablation products from polymers by picosecond-uv-laser mass spectroscopy. Applied Physics B, Photophysics and Laser Chemistry, 1987, 42, 181-184.	1.5	81
9	Atomic oxygen functionalization of double walled C nanotubes. Carbon, 2009, 47, 2579-2589.	10.3	79
10	Sensing gases with carbon nanotubes: a review of the actual situation. Journal of Physics Condensed Matter, 2010, 22, 013001.	1.8	79
11	Nature of the Decrease of the Secondary-Electron Yield by Electron Bombardment and its Energy Dependence. Physical Review Letters, 2012, 109, 064801.	7.8	74
12	Transition metal carbides (MXenes) for efficient NiO-based inverted perovskite solar cells. Nano Energy, 2021, 82, 105771.	16.0	74
13	Impact of Defects on the Surface Chemistry of ZnO(0001Ì")â^'O. Journal of the American Chemical Society, 2002, 124, 7117-7122.	13.7	73
14	Graphene-Induced Substrate Decoupling and Ideal Doping of a Self-Assembled Iron-phthalocyanine Single Layer. Journal of Physical Chemistry C, 2013, 117, 3019-3027.	3.1	71
15	Insulating Ground State ofSn/Si(111)â^'(3×3)R30°. Physical Review Letters, 2007, 98, 126401.	7.8	70
16	Epitaxial Growth of Hexagonal Boron Nitride on Ir(111). Journal of Physical Chemistry C, 2012, 116, 157-164.	3.1	69
17	Controlling Hydrogenation of Graphene on Ir(111). ACS Nano, 2013, 7, 3823-3832.	14.6	69
18	Epitaxial growth of single-orientation high-quality MoS <sub>2</sub> monolayers. 2D Materials, 2018, 5, 035012.	4.4	65

#	Article	IF	CITATIONS
19	A synchrotron radiation photoemission study of the oxidation of tin. Surface Science, 1994, 313, 379-391.	1.9	64
20	Epitaxial Growth of a Single-Domain Hexagonal Boron Nitride Monolayer. ACS Nano, 2014, 8, 12063-12070.	14.6	64
21	Unveiling the Mechanisms Leading to H <sub>2</sub> Production Promoted by Water Decomposition on Epitaxial Graphene at Room Temperature. ACS Nano, 2016, 10, 4543-4549.	14.6	60
22	The comparative XPS and PYS studies of SnO2 thin films prepared by L-CVD technique and exposed to oxygen and hydrogen. Sensors and Actuators B: Chemical, 2000, 70, 177-181.	7.8	57
23	Spectroscopic characterization of contaminants and interaction with gases in single-walled carbon nanotubes. Carbon, 2004, 42, 2099-2112.	10.3	51
24	Local Electronic Structure and Density of Edge and Facet Atoms at Rh Nanoclusters Self-Assembled on a Graphene Template. ACS Nano, 2012, 6, 3034-3043.	14.6	49
25	Band dispersion in the deep 1s core level ofÂgraphene. Nature Physics, 2010, 6, 345-349.	16.7	48
26	The secondary electron yield of noble metal surfaces. AIP Advances, 2017, 7, .	1.3	46
27	Electronic structure and molecular orientation of a Zn-tetra-phenyl porphyrin multilayer on Si(111). Surface Science, 2006, 600, 4013-4017.	1.9	44
28	Fine tuning of graphene-metal adhesion by surface alloying. Scientific Reports, 2013, 3, 2430.	3.3	43
29	ldentification of the Si2pSurface Core Level Shifts on theSb/Si(001)â^'(2×1)Interface. Physical Review Letters, 1998, 81, 2320-2323.	7.8	41
30	Mesoscopic Donorâ^'Acceptor Multilayer by Ultrahigh-Vacuum Codeposition of Zn-Tetraphenyl-Porphyrin and C70. Journal of the American Chemical Society, 2009, 131, 644-652.	13.7	41
31	Organotin films deposited by laser-induced CVD as active layers in chemical gas sensors. Thin Solid Films, 1998, 323, 291-295.	1.8	40
32	Detailed investigation of the low energy secondary electron yield of technical Cu and its relevance for the LHC. Physical Review Special Topics: Accelerators and Beams, 2015, 18, .	1.8	39
33	X-ray photoelectron microscopy of the C 1s core level of free-standing single-wall carbon nanotube bundles. Applied Physics Letters, 2002, 80, 2165-2167.	3.3	38
34	Secondary electron yield of Cu technical surfaces: Dependence on electron irradiation. Physical Review Special Topics: Accelerators and Beams, 2013, 16, .	1.8	38
35	Bottom-up approach for the low-cost synthesis of graphene-alumina nanosheet interfaces using bimetallic alloys. Nature Communications, 2014, 5, 5062.	12.8	37
36	lon Implantation as an Approach for Structural Modifications and Functionalization of Ti <sub>3</sub> C <sub>2</sub> T <sub><i>x</i>&gt;/sub&gt; MXenes. ACS Nano, 2021, 15, 4245-4255.</sub>	14.6	37

#	Article	IF	CITATIONS
37	Self-Assembly of Graphene Nanoblisters Sealed to a Bare Metal Surface. Nano Letters, 2016, 16, 1808-1817.	9.1	36
38	Electron accumulation layer on clean In-terminated InAs(0 0 1)(4×2)-c(8×2) surface. Surface Science, 2001, 482-485, 587-592.	1.9	35
39	Metal-phthalocyanine array on the moiré pattern of a graphene sheet. Journal of Nanoparticle Research, 2011, 13, 6013-6020.	1.9	33
40	Structural reorganization of carbon nanoparticles into single-wall nanotubes. Physical Review B, 2002, 66, .	3.2	32
41	Illuminating the earliest stages of the soot formation by photoemission and Raman spectroscopy. Combustion and Flame, 2017, 181, 188-197.	5.2	32
42	Reduction and shaping of graphene-oxide by laser-printing for controlled bone tissue regeneration and bacterial killing. 2D Materials, 2018, 5, 015027.	4.4	32
43	The photochemistry of CH4 adsorbed on Pt(1 1 1) studied by high resolution fast XPS. Surface Science, 2001, 482-485, 134-140.	1.9	30
44	The Role of Metal Contact in the Sensitivity of Single-Walled Carbon Nanotubes to NO <sub>2</sub> . Journal of Physical Chemistry C, 2007, 111, 12169-12174.	3.1	30
45	Evolution of the secondary electron emission during the graphitization of thin C films. Applied Surface Science, 2015, 328, 356-360.	6.1	29
46	Surface analysis study of the oxidation of organotin films deposited by ArF excimer laser chemical vapor deposition. Journal of Vacuum Science and Technology A: Vacuum, Surfaces and Films, 1997, 15, 2492-2501.	2.1	28
47	Energy dependence of resonant charge transfer from adsorbates to metal substrates. Chemical Physics, 2003, 289, 107-115.	1.9	28
48	Direct writing of fluorescent patterns on LiF films by x-ray microprobe. Applied Physics Letters, 2002, 80, 3862-3864.	3.3	27
49	Interface formation between C60 and diethynyl-Zn-porphyrinato investigated by SR-induced photoelectron and near-edge X-ray absorption (NEXAFS) spectroscopies. Chemical Physics, 2004, 297, 307-314.	1.9	27
50	Double perovskite Sr2FeMoO6 films: Growth, structure, and magnetic behavior. Journal of Applied Physics, 2006, 100, 013907.	2.5	27
51	Molecular orientations, electronic properties and charge transfer timescale in a Zn-porphyrin/C70 donor–acceptor complex for solar cells. Surface Science, 2006, 600, 4018-4023.	1.9	26
52	Key role of rotated domains in oxygen intercalation at graphene on Ni(1 1 1). 2D Materials, 2017, 4, 025106.	4.4	26
53	Epitaxial growth of MgB2(0001) thin films on magnesium single-crystals. Applied Physics Letters, 2004, 85, 976-978.	3.3	24
54	The electronic properties of carbon nanotubes studied by high resolution photoemission spectroscopy. Applied Surface Science, 2005, 248, 8-13.	6.1	24

#	Article	IF	CITATIONS
55	Molecular adsorption and multilayer growth of pentacene on Cu(100): Layer structure and energetics. Physical Review B, 2007, 75, .	3.2	24
56	Substrate Influence for the Znâ€ŧetraphenylâ€porphyrin Adsorption Geometry and the Interfaceâ€induced Electron Transfer. ChemPhysChem, 2010, 11, 2248-2255.	2.1	24
57	Multiple-photon excitation spectra of SiH4 measured in the 10 μm range by a continuously tunable CO2 laser. Chemical Physics Letters, 1985, 122, 480-488.	2.6	23
58	On the hydrophilic/hydrophobic character of carbonaceous nanoparticles formed in laminar premixed flames. Experimental Thermal and Fluid Science, 2016, 73, 56-63.	2.7	23
59	Synthesis of nitrogen-doped epitaxial graphene via plasma-assisted method: Role of the graphene–substrate interaction. Surface Science, 2016, 643, 214-221.	1.9	22
60	Spin-dependent electron-phonon coupling in the valence band of single-layer <mml:math xmlns:mml="http://www.w3.org/1998/Math/MathML"&gt; <mml:msub> <mml:mi>WS </mml:mi> <mml:mn>2 Physical Review B, 2017, 96, .</mml:mn></mml:msub></mml:math 	mn <b>3.</b> 2/mm	າl:m2s2ub>
61	Secondary electron emission and yield spectra of metals from Monte Carlo simulations and experiments. Journal of Physics Condensed Matter, 2019, 31, 055901.	1.8	22
62	A fast XPS study of sulphate promoted propene decomposition over Pt{}. Surface Science, 2002, 513, 140-148.	1.9	21
63	Transition from one-dimensional to three-dimensional behavior induced by lithium doping in single wall carbon nanotubes. Physical Review B, 2005, 71, .	3.2	20
64	Synchrotron radiation photoemission analysis of ArF laser deposited tin oxide. Journal of Vacuum Science and Technology A: Vacuum, Surfaces and Films, 1993, 11, 336-340.	2.1	19
65	<mml:math display="inline" xmlns:mml="http://www.w3.org/1998/Math/MathML"><mml:mrow><mml:mi mathvariant="normal"&gt;C<mml:mspace <br="" width="0.2em">/&gt;<mml:mn>1</mml:mn><mml:mi>s</mml:mi></mml:mspace></mml:mi </mml:mrow></mml:math> photoemission spectrum in graphite(0001). Physical Review B, 2007, 76, .	3.2	19
66	Bulk sensitive x-ray absorption and magnetic circular dichroism investigation of Mn- and Co-doped ZnO thin films. Applied Physics Letters, 2010, 97, 052505.	3.3	19
67	Photoemission investigation of oxygen intercalated epitaxial graphene on Ru(0001). Surface Science, 2018, 678, 57-64.	1.9	18
68	Growth and structure of singly oriented single-layer tungsten disulfide on Au(111). Physical Review Materials, 2019, 3, .	2.4	18
69	KrF-excimer-laser-induced native oxide removal from Si (100) surfaces studied by Auger electron spectroscopy. Applied Physics A: Materials Science and Processing, 1996, 62, 103-114.	2.3	17
70	Electron transfer fromGdions to theCcage in endohedralGd@C82probed by resonant photoemission spectroscopy. Physical Review B, 2004, 70, .	3.2	17
71	Excimer-laser-induced photochemistry of organometallic compounds monitored by dye laser mass spectroscopy: dimethyl ditelluride (CH3TeTeCH3). The Journal of Physical Chemistry, 1986, 90, 4568-4573.	2.9	16
72	C70 adsorbed on Cu(111): Metallic character and molecular orientation. Journal of Chemical Physics, 2002. 116. 7685-7690.	3.0	16

#	Article	IF	CITATIONS
73	Core Level Photoemission Evidence of Frustrated Surface Molecules: A Germ of Disorder at the (111) Surface ofC60before the Order-Disorder Surface Phase Transition. Physical Review Letters, 2002, 88, 196102.	7.8	16
74	Electronic properties of clean and Li-doped single-walled carbon nanotubes. Journal of Electron Spectroscopy and Related Phenomena, 2005, 144-147, 793-797.	1.7	16
75	Ultrafast Charge Transfer at Monolayer Graphene Surfaces with Varied Substrate Coupling. ACS Nano, 2013, 7, 4359-4366.	14.6	16
76	On the compatibility of porous surfaces with cryogenic vacuum in future high-energy particle accelerators. Applied Physics Letters, 2019, 114, .	3.3	16
77	High resolution electron microscopy and x-ray photoelectron spectroscopy studies of heteroepitaxial SixGe(1â~x) alloys produced through laser induced processing. Applied Physics Letters, 1998, 72, 2877-2879.	3.3	15
78	Vibrational and electronic properties of hydrogen adsorbed on single-wall carbon nanotubes. Physical Review B, 2004, 69, .	3.2	15
79	Local and long-range order of carbon impurities on Fe(100): Analysis of self-organization at a nanometer scale. Physical Review B, 2006, 73, .	3.2	15
80	Synchrotron radiation photoelectron spectroscopy of the O(2s) core level as a tool for monitoring the reducing effects of ion bombardment on SnO2 thin films. Applied Surface Science, 1996, 104-105, 349-353.	6.1	14
81	Characterization of high-quality MgB2(0001) epitaxial films on Mg(0001). New Journal of Physics, 2006, 8, 12-12.	2.9	14
82	Mixed Cation Halide Perovskite under Environmental and Physical Stress. Materials, 2021, 14, 3954.	2.9	14
83	Excimer laser photolysis of organometallic compounds monitored by laser mass spectroscopy. Journal of Crystal Growth, 1986, 77, 235-240.	1.5	13
84	Morphology and magnetic properties of thin films of Rh on highly oriented pyrolitic graphite. Physical Review B, 2000, 63, .	3.2	13
85	Localization of3delectrons in thin Mn and Mn-oxide films by resonant photoemission. Physical Review B, 2001, 63, .	3.2	13
86	A Fast XPS Study of Propene Decomposition over Clean and Sulphated Pt{111}. Catalysis Letters, 2002, 78, 379-382.	2.6	13
87	Electronic and vibrational excitations in carbon nanotubes. Carbon, 2003, 41, 985-992.	10.3	13
88	Thermal reactions at the interface between Si and C nanoparticles: nanotube self-assembling and transformation into SiC. Surface Science, 2003, 532-535, 886-891.	1.9	13
89	Calorimetry at Surfaces Using High-Resolution Core-Level Photoemission. Physical Review Letters, 2004, 93, 106105.	7.8	13
90	NO2 decomposition on Rh clusters supported on single-walled carbon nanotubes. Applied Physics Letters, 2006, 88, 243111.	3.3	13

#	Article	IF	CITATIONS
91	Chemical gating of epitaxial graphene through ultrathin oxide layers. Nanoscale, 2015, 7, 12650-12658.	5.6	13
92	The adsorption of silicon on an iridium surface ruling out silicene growth. Nanoscale, 2018, 10, 7085-7094.	5.6	13
93	Excimer laser cleaning of Si(100) surfaces at 193 and 248 nm studied by LEED, AES and XPS spectroscopies. Journal of Electron Spectroscopy and Related Phenomena, 1995, 76, 607-612.	1.7	12
94	X-ray diffraction and x-ray photoelectron spectroscopy study of partially strained SiGe layers produced via excimer laser processing. Journal of Applied Physics, 1997, 82, 147-154.	2.5	12
95	Thermal and pulsed laser induced surface reactions in Ti/Si(001) interfaces studied by spectromicroscopy with synchrotron radiation. Journal of Applied Physics, 2001, 90, 4361-4369.	2.5	12
96	Occupied density of states inMgB2revealed by photoemission microscopy. Physical Review B, 2002, 66, .	3.2	12
97	ArF excimer laser deposited tin oxide films studied by "in situ―surface diagnostics and by synchrotron radiation induced UV photoemission. Applied Surface Science, 1993, 69, 59-64.	6.1	11
98	Silicon nanowires grown on Si(100) substrates via thermal reactions with carbon nanoparticles. Chemical Physics Letters, 2003, 371, 394-400.	2.6	11
99	Charge transfer from core-excited argon adsorbed on clean and hydrogenated Si(100): ultrashort timescales and energetic structure. New Journal of Physics, 2009, 11, 053005.	2.9	11
100	Effect of the surface processing on the secondary electron yield of Al alloy samples. Physical Review Special Topics: Accelerators and Beams, 2013, 16, .	1.8	11
101	Unexpected Rotamerism at the Origin of a Chessboard Supramolecular Assembly of Ruthenium Phthalocyanine. Chemistry - A European Journal, 2017, 23, 16319-16327.	3.3	11
102	Photoprocesses in organometallics. Applied Surface Science, 1990, 46, 19-26.	6.1	10
103	Bis(triisopropylsilylethynyl)pentacene/Au(111) Interface: Coupling, Molecular Orientation, and Thermal Stability. Journal of Physical Chemistry C, 2014, 118, 22522-22532.	3.1	10
104	ArF excimer laser epitaxy of SixGe1â^'x alloys studied by XRD and XPS. Applied Surface Science, 1996, 106, 179-185.	6.1	9
105	TRACKING THERMALLY DRIVEN MOLECULAR REACTION AND FRAGMENTATION BY FAST PHOTOEMISSION: C60on Si(111). Surface Review and Letters, 2002, 09, 775-781.	1.1	9
106	Final-state screening dynamics in resonant Auger decay at the2pedge of vanadium. Physical Review B, 2005, 71, .	3.2	9
107	Minimum thickness of carbon coating for multipacting suppression. Physical Review Research, 2020, 2,	3.6	9
108	Laser multiphoton mass spectroscopy of zinc dialkyls. Chemical Physics Letters, 1988, 147, 161-167.	2.6	8

#	Article	IF	CITATIONS
109	Laser-induced integrated processing for heteroepitaxial SixGe(1â^'x) alloys. Applied Surface Science, 1996, 102, 42-46.	6.1	8
110	Growth of Ge layers on Si(100) monitored by in situ ellipsometry. Thin Solid Films, 1998, 315, 49-56.	1.8	8
111	Evaluation of alkali-induced band-bending inhomogeneity and charge transfer trend from core-level analysis. Physical Review B, 2000, 62, R10657-R10660.	3.2	8
112	Ge/Si(001)c(4×2)interface formation studied by high-resolution Ge3dand Si2pcore-level spectroscopy. Physical Review B, 2000, 61, 16006-16014.	3.2	8
113	Carbon nanotube bundles and thin layers probed by micro-Raman spectroscopy. European Physical Journal B, 2003, 31, 203-208.	1.5	8
114	Fundamental Role of the H-Bond Interaction in the Dissociation ofNH3onSi(001)â^'(2×1). Physical Review Letters, 2012, 109, 036102.	7.8	8
115	The effect of structural disorder on the secondary electron emission of graphite. AIP Advances, 2016, 6, .	1.3	8
116	Dual-Route Hydrogenation of the Graphene/Ni Interface. ACS Nano, 2019, 13, 1828-1838.	14.6	8
117	Laser-induced dissociation of polychlorinated biphenyls in the liquid phase. Chemical Physics Letters, 1988, 143, 245-250.	2.6	7
118	Excimer laser photolysis of organometallic compounds for Zn deposition. Applied Surface Science, 1989, 36, 221-230.	6.1	7
119	Cr, Sn and interface formation studied by synchrotron radiation induced UPS. Journal of Electron Spectroscopy and Related Phenomena, 1995, 76, 499-504.	1.7	7
120	UHV-CVD Ge/Si(100) heteroepitaxy monitored by in situ ellipsometry. Applied Surface Science, 1996, 102, 52-56.	6.1	7
121	A Spectroscopic and ab Initio Study of the Formation of Graphite and Carbon Nanotubes from Thermal Decomposition of Silicon Carbide. Nano Letters, 2008, 8, 4335-4341.	9.1	7
122	Electron–phonon coupling in single-layer MoS2. Surface Science, 2019, 681, 64-69.	1.9	7
123	Tuning the charge state of a C60 single layer on Ag(1 0 0) by Na deposition. Surface Science, 2001, 482-485, 606-611.	1.9	6
124	Electron microscopy and photoelectron spectromicroscopy study of catalyst-free transformation of carbon nanoparticles into nanotubes. Journal of Applied Physics, 2005, 98, 084307.	2.5	6
125	Electronic surface reconstruction and correlation in the fcc and dimer phases ofRbC60. Physical Review B, 2007, 75, .	3.2	6
126	Interaction of molecular oxygen with single wall nanotubes: Role of surfactant contamination. Nuclear Instruments & Methods in Physics Research B, 2003, 200, 5-10.	1.4	5

#	Article	IF	CITATIONS
127	Spectroscopic characterization of contaminants and interaction with gases in single-walled carbon nanotubes. Carbon, 2004, 42, 2099-2099.	10.3	5
128	Search for a local effect in multiatom resonant core excitation in a surface species: Photoemission and photon-stimulated desorption fromN2on Ni(111). Physical Review B, 2005, 71, .	3.2	5
129	Electronic properties of a pure and sodium-doped C70 single layer adsorbed on Al polycrystalline surface. Journal of Chemical Physics, 2005, 122, 054704.	3.0	5
130	Isotope selective ionization of tellurium dimers Te2 formed by excimer laser photodissociation of an organometallic compound: CH3TeTeCH3. Applied Physics B, Photophysics and Laser Chemistry, 1986, 41, 213-215.	1.5	4
131	Ge/Bi/Si(001)-c(4×2) interface studied by high-resolution core-level spectroscopy. Surface Science, 1999, 433-435, 362-366.	1.9	4
132	Lateral heterogeneity in the surface composition after laser processing of Ti/Si interface contaminated with oxygen. Applied Physics Letters, 2001, 79, 191-193.	3.3	4
133	Metallic phases of a C70 single layer adsorbed on Cu(111) doped with sodium. Surface Science, 2003, 532-535, 892-897.	1.9	4
134	Luminescent nanostructures based on colour centres produced in LiF films by direct writing with an X-ray microprobe. Physica Status Solidi C: Current Topics in Solid State Physics, 2005, 2, 298-301.	0.8	4
135	Detailed Investigation of the Low-Energy Secondary Electron Yield (LE-SEY) of Clean Polycrystalline Cu and of Its Technical Counterpart. IEEE Transactions on Plasma Science, 2015, 43, 2954-2960.	1.3	4
136	SEY and low-energy SEY of conductive surfaces. Journal of Electron Spectroscopy and Related Phenomena, 2020, 241, 146876.	1.7	4
137	Impact of the Substrate Work Function on Self-Assembling and Electronic Structure of Adsorbed Ruthenium Phthalocyanine. Journal of Physical Chemistry C, 2020, 124, 23295-23306.	3.1	4
138	Visible and UV pulsed laser processing of the Ti/Si(0 0 1) interface studied by XPS microscopy with synchrotron radiation. Surface Science, 2001, 482-485, 141-146.	1.9	3
139	ANGLE-SCANNED PHOTOELECTRON DIFFRACTION: FROM CLEAN SURFACES TO COMPLEX ADSORPTION SYSTEMS. Surface Review and Letters, 2002, 09, 741-747.	1.1	3
140	Ultra-high-vacuum epitaxial growth of MgB2(0001) thin films on Mg(0001) via molecular beam epitaxy. Journal of Physics Condensed Matter, 2004, 16, S3451-S3458.	1.8	3
141	Space and time resolved emission spectroscopy of Sr2FeMoO6 laser induced plasma. Applied Surface Science, 2005, 248, 19-23.	6.1	3
142	Microstructure and magnetic behavior of PLD Sr2FeMoO6 thin films. Physica Status Solidi C: Current Topics in Solid State Physics, 2006, 3, 3229-3232.	0.8	3
143	Graphene-based field effect transistors for radiation-induced field sensing. Nuclear Instruments and Methods in Physics Research, Section A: Accelerators, Spectrometers, Detectors and Associated Equipment, 2016, 824, 392-393.	1.6	3
144	Excimer laser photolysis of Zn dialkyls for Zn deposition. Nuovo Cimento Della Societa Italiana Di Fisica D - Condensed Matter, Atomic, Molecular and Chemical Physics, Biophysics, 1989, 11, 1603-1613.	0.4	2

#	Article	IF	CITATIONS
145	Resonant production of doubly charged tin ions in the multiphoton ionization of tin alkyls. Chemical Physics Letters, 1992, 199, 605-608.	2.6	2
146	Temperature effect on the reconstruction of Sb/Si(001) interface studied by high resolution core level spectroscopy and RHEED analysis. Applied Surface Science, 2000, 166, 214-219.	6.1	2
147	Advanced optical characterization of active micro-strips induced on Lithium Fluoride crystals by a monochromatic soft X-ray beam. Journal of Non-Crystalline Solids, 2007, 353, 456-460.	3.1	2
148	Soft X-ray imaging by optically stimulated luminescence from color centers in lithium fluoride. Spectrochimica Acta, Part B: Atomic Spectroscopy, 2007, 62, 631-635.	2.9	2
149	Substrate-Driven Formation of Bidimensional Arrays of Co Nanocrystals in TiO <sub>2</sub> Thin Films. Journal of Physical Chemistry C, 2013, 117, 687-691.	3.1	2
150	Combined high resolution X-ray diffraction and EXAFS studies of Si(1â^'x)Gex heterostructures. Thin Solid Films, 1998, 319, 20-24.	1.8	1
151	De Padovaet al.Reply:. Physical Review Letters, 1999, 82, 4565-4565.	7.8	1
152	<title>ArF excimer laser photolysis of tetramethyltin Sn(CH3)4 probed by dye-laser-induced resonant&lt;br&gt;multiphoton ionization</title> . , 1990, 1279, 170.		0
153	Multiphoton dissociation of zinc dialkyls probed by resonance-enhanced multiphoton ionization. Chemical Physics Letters, 1993, 203, 15-20.	2.6	0
154	CVD Growth and Excimer Laser Processing of SiGe Alloys Monitored by Single Wavelength Ellipsometry and Atomic Force Microscopy. Materials Research Society Symposia Proceedings, 1997, 502, 65.	0.1	0
155	Bulk-likeSi(001) atomic rearrangement artificially created at theGe/Sb/Si(001) interface. Nuovo Cimento Della Societa Italiana Di Fisica D - Condensed Matter, Atomic, Molecular and Chemical Physics, Biophysics, 1998, 20, 1029-1037.	0.4	0
156	High resolution photoemission core level spectroscopy study and TEM analysis of the Ge/As/Si(0 0 1) growth. Surface Science, 2001, 482-485, 574-579.	1.9	0
157	<title>Laser ablated&lt;br&gt;Sr&lt;formula&gt;&lt;inf&gt;&lt;roman&gt;2&lt;/roman&gt;&lt;/inf&gt;&lt;/formula&gt;FeMoO&lt;formula&gt;&lt;inf&gt;&lt;roman&gt;6&lt;/roman&gt;&lt;/inf&gt;&lt;/formula&lt;br&gt;plasma studied by optical emission spectroscopy</title> ., 2005, , .	a>	0
158	<title>Direct writing of luminescent nanostructures in lithium fluoride films by x-ray microprobe scanning</title> . , 2005, , .		0
159	Spectroscopic Characterization of Flame-Generated 2-D Carbon Nano-Disks. Materials Research Society Symposia Proceedings, 2015, 1726, 56.	0.1	0
160	Crystal to Quasicrystal Surface Phase Transition: An Unlocking Mechanism for Templated Growth. Journal of Physical Chemistry C, 2016, 120, 5477-5485.	3.1	0
161	Gas and Adsorbed-Phase UV Photochemistry of Tetramethyltin (TMT) Probed by In-Situ Optical Diagnostics and Surface-Sensitive Techniques. , 1994, , 133-151.		0
162	Producción y tratamiento de pelÃculas de Si <sub>1-x</sub> Ge <sub>x</sub> mediante técnicas asistidas por láser de excÃmero. Revista De Metalurgia, 1998, 34, 78-81.	0.5	0

#	Article	IF	CITATIONS
163	KrF-excimer-laser-induced native oxide removal from Si(100) surfaces studied by Auger electron spectroscopy. Applied Physics A: Materials Science and Processing, 1996, 62, 103-114.	2.3	0